Revista Brasileira de Aplicações de Vácuo, v. 22, n. 2, 39-44, 2003.

VACUUM SYSTEM OF HIGH-ENERGY ACCELERATORS: ELECTRICAL BREAKDOWN IN VACUUM

Y.Saito
KEK-High Energy Accelerator Research Organization
Tsukuba, Ibaraki, 305 Japan

Keywords: accelerator, electrical breakdown, outgassing

ABSTRACT

Accelerator component materials, such as oxygen-free copper, alumina ceramics and stainless steels to be installed in a vacuum must necessarily be chosen and treated so as not to induce an electrical breakdown. Some R&D work carried out at KEK concerning the breakdown characteristics of several materials and treatments is reported. Hydrogen molecules that are absorbed in the copper bulk as well as surface contamination influence its breakdown strength when used as an electrode. Surface finishing by diamond turning of the copper electrodes has been examined. As for the alumina ceramics used as an electrical insulator, micro voids and sintering additives in the material cause breakdown and surface melting when multipactoring takes place. Oxygen defects in alumina are strongly related to its durability under a high electric field. Outgassing, which may induce breakdown phenomena, have also been measured for some components for in-vacuum use.

1. INTRODUCTION

The KEK accelerator system involves the electron and positron linacs for 7.5 and 3.5 GeV, respectively, the Photon Factory, the electron-positron colliding ring (KEKB) and the proton synchrotron ring of 12 GeV. We have some serious breakdown problems in the accelerator components, especially when installed in a vacuum. Arcing in the electron gun and rf window breakdown often take place in a 50 MW klystron used for the electron linac. The accelerating structure of the electron linac, in which 2856 MHz rf power is being fed, sometimes showed breakdown even when it was operated with an electric field of about 12 MV/m. The proton linac also has a breakdown problem in the 200 MHz standing-wave cavity, in which the electric field is less than several MV/m.
In order to suppress these breakdowns, it is necessary to know the breakdown characteristics, how to choose the materials, and how to process the material surfaces. Several R&D projects have been carried out concerning the breakdown characteristics of metal electrodes and alumina insulator surfaces. It is important not only to clean the surfaces of all high-voltage components, but also to reduce outgassing from all of the components in a vacuum so as to suppress the breakdown phenomena. The outgassing rates were measured for surface-treated stainless-steels, several kinds of co-axial cables and laminated magnetic cores.

2. BREAKDOWN CHARACTERISTICS OF METAL ELECTRODES

2.1. OXYGEN-FREE-COPPER

Oxygen-free-copper (OFC) is graded according to its purity, and the highest grade for industrial materials, having a purity of up to 99.99%, is, further, specified and classified into 5 classes by ASTM-F-68 according to the micro structure. The hydrogen content is strongly related to the micro-void in the grain.[1] A gas chromatographic analysis, indeed, shows a difference in the hydrogen content; the class-1 and class-5 contain 0.3 and 0.8 ppm of hydrogen, respectively. The influence of the hydrogen contents on the gap-breakdown characteristics of OFC electrodes (18 mm in diameter) was examined by applying an impulse voltage of 700 μs[2]. Before testing, pre-cleaning was carried out using Ar+ beam sputtering with 3 keV, 2 mA. An electrode of OFC Class-1, having smaller hydrogen content, showed a better performance during the conditioning process involving a repetitive application of impulse voltages, and thus has higher breakdown strength than do the class-5 OFC electrodes. This indicates that hydrogen atoms, which are absorbed in the anode copper bulk, are possibly desorbed and ionized, and then cause a breakdown when emitted electrons from the cathode are irradiated on the anode.
The gap-breakdown strength, as is well known, is strongly influenced by the surface finishing procedures applied to the electrodes. Generally, electrode surfaces are machined or polished to be smooth, since any surface protrusion may cause electron emission, which induces breakdown. Polishing or machining, however, sometimes increases the surface residual stresses, which tend to affect the field-emission characteristics. The methods of "electrochemical buffing[3]" and "diamond turning" are used to produce a mirror-finish surface without introducing any surface stresses,[2] since unnecessary forces are not applied to the surface during processing. Indeed, both treatments are effective to shorten the conditioning periods, as shown in Fig.1, than normal machining by an ordinal lathe. Further, electrodes finished by diamond turning show a higher value in breakdown strength after conditioning; an electrochemically buffed surface, showing a fast rising of the breakdown field, but not showing a significant increase, is likely to include some chemical compounds which may induce electron emission. It is considered that a diamond turning finish has less residual stress and, also, that the surface is chemically stable.

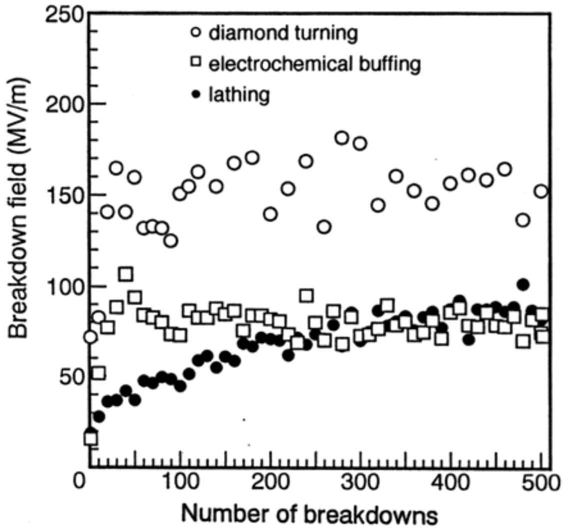

Figure 1 - Conditioning characteristics observed for electrodes finished by diamond turning, electrochemical polishing and, ordinal lathe work.

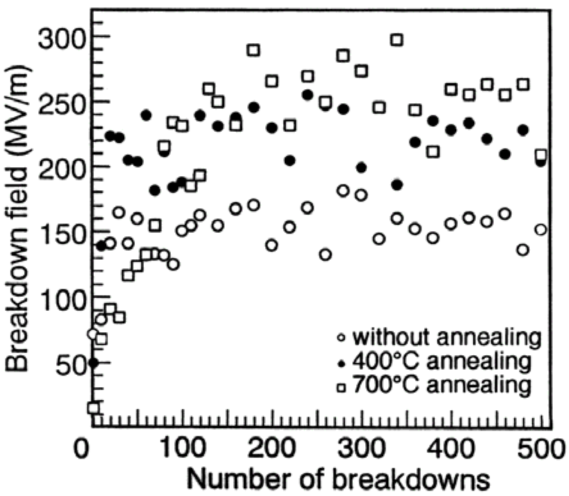

Figure 2 - Annealing effect on the breakdown strength. The electrodes were finished by diamond turning after annealing.

Figure 2 shows the breakdown strengths observed for in-vacuum annealed electrodes (OFC Class-1). The electrodes were annealed at temperatures of 400 and 700C; after annealing, the observed surface residual stress became higher (tensile) as the heating temperature was increased, but was then reduced by diamond turning.[2] The breakdown strength is clearly increased by annealing at a higher temperature. This indicates that further outgassing of Class-1 copper suppresses breakdown when the surface stress is sufficiently reduced by diamond turning. It is pointed out that without surface finishing by diamond turning the breakdown field of the electrode was only 150 MV/m, even after it had been annealed at 700C.[2]

2.2. ALUMINUM

An aluminum material is often used in accelerator vacuum components as a gasket or a beam duct; it is further used for a kicker magnet electrode having a large area because of its lightweight and good conductivity. A practically roll-finished surface of aluminum is degraded and has a porous oxide layer, which is chemically unstable to adsorb water molecules. Electropolishing is one of the techniques used to remove such a degraded surface and to stabilize the aluminum surfaces chemically. However, hydrogen gas bubbles in an electrolyte solution easily cause surface pits on the aluminum surface; selective etching takes place where a bubble is adsorbed. Recently, a pit-free electropolishing method has been developed; strongly agitating the solution and controlling the flow direction are effective to remove the hydrogen.[4] The surface of rf waveguide gaskets polished by this method was optically flat and the roughness was measured to be less than 0.03 μm on the average.

From a depth-profile analysis by AES observation, the surface was found to be covered by an oxide layer (200 nm thick[4]); a naturally formed oxide layer on an aluminum surface is of the order of nm. Because this layer formed in an electrolyte solution is considered not to be porous, it is stable. In fact, the true surface area measured by the BET (Brewer-Emette-Tayler) method is nearly equal to a geometrical surface area, while that of an anodized aluminum surface is 200-times the geometric surface area. Further, the outgassing rate measured for an electropolished surface shows a very low value of 10^{-10} Pa m s^{-1}. When electropolishing is applied to the surface of an aluminum electrode, it is expected to have a good performance in the HV conditioning process. The breakdown field strength observed for an impulse voltage application was 150 MV/m, which is higher than that of an unpolished electrode (80 MW/m), as shown in Fig.3.[5] We applied this method to a capacitor electrode of the kicker magnet for use in the 12 GeV-proton fast-extraction system (Fig.4), and have operated it successfully, so far.

3. BREAKDOWN CHARACTERISTICS OF INSULATOR SURFACES

3.1. MULTIPACTOR-INDUCED SURFACE MELTING

Since an alumina ceramic material has a low outgassing rate and is durable under a heat treatment, it is widely used in accelerator vacuum systems as electrical insulators, such as cavity input couplers and high-voltage sealing. The failure of alumina rf windows in high-power klystrons is one of the most serious problems.[6] In the S-band 30 MW klystron used at KEK, the breakdown of a pillbox-type window is mainly caused by multipactor electron bombardment[7] due to a high yield of the secondary electron emission of the alumina ceramics.

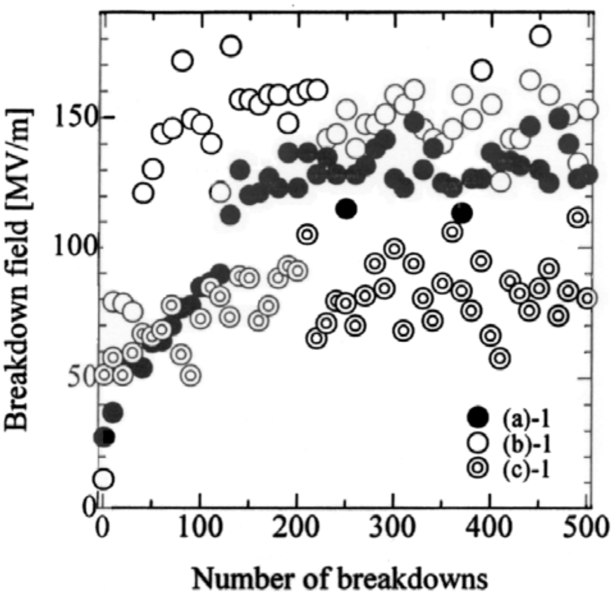

Figure 3 - Effect of pit-free electropolishing on the aluminum electrodes gap-breakdown. The periods of electropolishing of (a)-1 and (b)-1 are 10 and 5 min, respectively. (c)-1 was not electropolished.

Once multipactoring takes place on an alumina ceramic surface, optical emission from the surface can be seen during rf operation, and after some operation period the surface becomes melted and cracked. The optical emission resulting from electron multipactoring is a luminescence of the alumina, the spectrum of which has a structure with a broad band at about 300 nm and a line at 694 nm.[8] The latter can be identified as being the color of ruby attributed by Cr impurity, and the former is an F^+-center of the oxygen vacancy of alumina. It is to be further noted that an additional band at 410 nm always appears when surface melting starts to take place.[9]

The 410 nm peak in the spectrum is a luminescence, corresponding to an F-center of oxygen vacancy. The energy level of the F-center, in which two electrons are trapped, is very close to the conduction band. The electron in the F^+-center can be easily excited to be conductive, thus causing ohmic loss when an electric field is applied. On the other hand, an F^+-center, having one trapped electron in a deep energy level, is converted to the F-center when heated in a vacuum, that is to say without oxygen. The possible process of alumina surface melting induced by multipactoring is, therefore, as follows: once multipactoring takes place, electron bombardment heats the surface and produces F-centers, and then any rf loss due to the conductive electrons causes excessive heating of the surface. This run-away phenomenon is probably enhanced by other thermal processes due to ion conductionin sintering additives of grain boundaries, such as SiO_2 and MgO, and/or due to field enhancement in the void.

Several kinds of alumina ceramics, including single crystal of sapphire, have been examined for high-power rf operation (Table 1). A ceramic (HA-997), was specially sintered in order to crystallize boundary additives having a low loss-tangent. It shows higher durability under high-power operation, and is not liable for F-centers. On the contrary, sapphire, though having the lowest loss-tangent value, involves pre-existing F-centers and high secondary yield; it is not good in high-power performance. As for XKP-999, since it is sintered without using sintering additives, it is a high purity alumina ceramic. However there are some residual voids (micro-porosity), which, consequently, cause a high value of the loss-tangent. It is therefore concluded that high-purity alumina having a low loss-tangent, but having neither a void nor a pre-existing F-center, is durable under a high electric field.

3.2. TIN COATING

An effective method used to avoid detrimental breakdown in rf windows is to suppress multipactoring, as well as making a better choice of alumina materials, as described above. Surface coatings of some metallic compounds, especially TiN, having low yields of secondary electrons, are applicable. The secondary yield is strongly related to the electron mean-free-path (λ) in solids. Since λ is usually about 0.4 – 1 nm in a metal, while 50 – 100 nm in an insulator, the secondary electrons generated in alumina can be absorbed in an overcoated metallic film. The secondary yield decreases in a manner characterized by λ as $\exp(-t/\lambda)$, when they pass through a TiN film with a thickness of t. The secondary yields measured for alumina ceramics coated by TiN are shown in Fig. 5 as a function of incident electron energies. The drastic decrease in the yield observed as the thickness increases is due to a small value of λ (0.5 nm or more). Figure 6 shows the luminescence pattern observed during rf operation for the alumina disk where TiN films are coated with different thicknesses. Multipactoring is clearly suppressed by TiN coatings of 0.5 nm thick or more.

Table 1- High-power performance of alumina materials for rf window use.

alumina material	**purity** (%)	**specific** gravity	**ε**	**tan δ** (10^{-5})	**SEE** (10 keV)	**CLspectra** before op.	**CL spectra after op.** TiN	uncoated	**transmit.** Power (MW)
UHV-99	99.0	3.90	9.91	9.4	2.0	F^+, Cr^{+3}	F^+, Cr^{+3}	F^+, Cr^{+3}, F (coloring)	>220
HA-997	99.7	3.93	9.95	4.2	2.0	F^+, Cr^{+3}	F^+, Cr^{+3}	F^+, Cr^{+3} (none)	>220
XKP-999	99.9	3.91	9.67	13.3	2.2	F^+, Cr^{+3}	F^+, Cr^{+3}, F	F^+, Cr^{+3}, F (coloring)	144
sapphire	100	3.98	10.2	2.3	3.7	F^+, F	F^+, F (flashover)	F^+, F (melting)	75

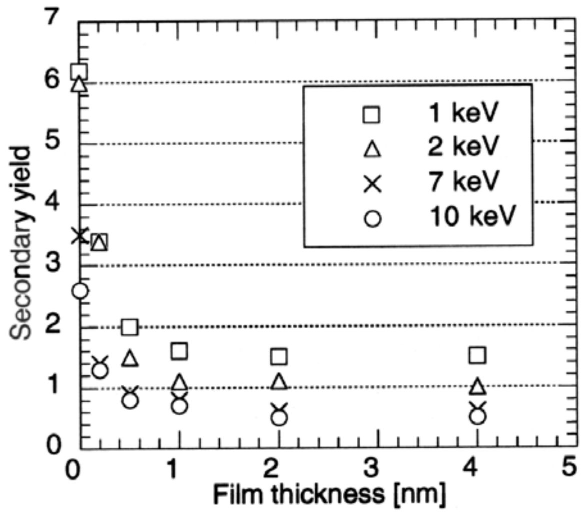

Figure 4 - Secondary electron emission yield of alumina ceramic TiN coated.

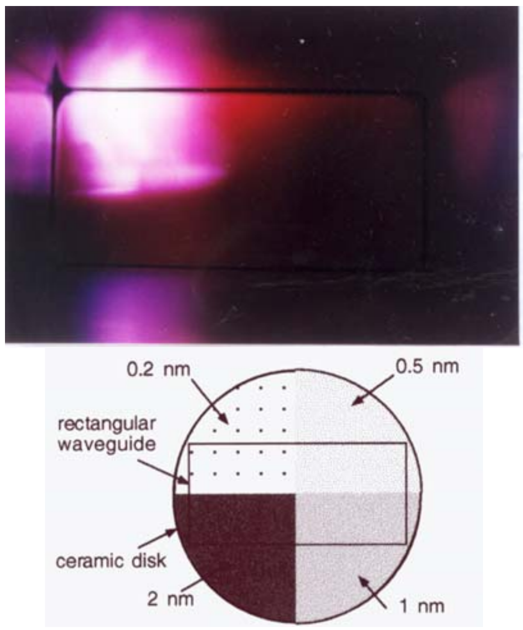

Figure 5 - Multipactor suppression by TiN coatings (27MW).

Since multipactor suppression coatings are electrically conductive, the films should be thin so as not to cause any excessive heating or surface flashover, although they should be sufficiently thick to reduce secondary electrons.[10]

3.3. SURFACE POLISHING AND ANNELING EFFECTS

Not only surface melting induced by multipactoring, but also momentary flashover accompanying outgassing, rf wave reflection and tree-like pattern of luminescence is characteristic of breakdown in rf windows (Fig.7). Occasional flashover in an alumina ceramic window takes place selectively on a TiN-coated surface during higher-power operation of 200 MW or more, corresponding to 8 kV/mm or more of the surface electric field. From *in-situ* measurements of surface charging before and after flashover,[11] several nC of positive charges are observed; tens of pC of negative or positive charges occur before flashover. This indicates a localized accumulation of electrons and a successive release as an avalanche across the surface, leaving positive charge.

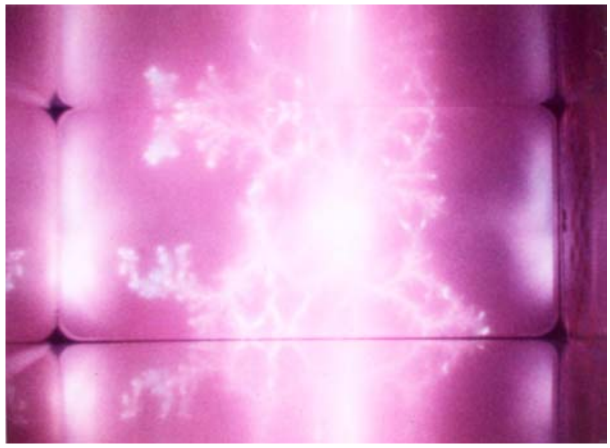

Figure 6 - Surface flashover observed in an RF window during 230 MW operation

The charge-accumulation mechanism is considered such that any mobile electrons that exist in F-centers and/or in conductive films are re-trapped in deeper energy levels of such defects of dislocations or microcracks in alumina ceramics. Mechanical polishing of the alumina surface, usually adopted as a finishing process, probably introduces surface residual stresses, which cause defects. In fact, unpolished alumina ceramics and sapphire disks show a higher durability than polished ones.[12] The flashover thresholds of polished disks have been increased by in-air annealing at 1500C, but do not reach to those of unpolished disks. The annealing treatment is, therefore, insufficient for eliminating all of the trapped sites; only the electronic states can probably be changed.[13]

4. OUTGASSING PROPERTIES

4.1. STAINLESS-STEEL

In order to reduce the outgassing rate of stainless-steel materials, several treatments have been proposed, such as vacuum firing and surface polishing. Using a conductance-modulation method[14], the outgassing rates have been measured for test ducts of 1 m long and 150 mm in diameter. The surfaces examined were pre-baked (550C in vacuum for 100h), TiN coated (1 μm thick film formed by hollow-cathode discharging) and electrochemically buffed (Rmax < 0.4 μm). The results are shown in Fig. 8.[15] The pre-baking method is expected to reduce the hydrogen content in the stainless-steel bulk, but is only effective after dry-nitrogen exposure. TiN film, being considered to be a barrier to hydrogen diffusion from the bulk to the surface, is effective to reduce water-molecule adsorption, probably due to its surface smoothness. Electrochemical buffing is a mirror-finish method used to eliminate the surface-degraded layer. The treated surface shows good performance, but not as passivated as a TiN-coated surface. However, this method is most advantageous for applying large components, because a large furnace or liquid reservoir is not necessary. Pure Ti material treated by oxidization in the surface outermost layer was also examined. The surface is likely to be sufficiently passivated to reduce outgassing, especially in a lower pressure region.

Some of these methods have been applied to accelerator vacuum systems. For example, the vacuum vessel for the PS fast-extraction kicker (1 x 2 x 1.5 m in dimension), was electrochemically buffed. The entire surface of the 300 m long duct (0.4 m dia.), has also been finished by electrochemical buffing. It is used for the laser interferometer for gravitational wave detection; the system pressure has reached in the range of 1 x 10^{-6} Pa without baking.[16]

4.2. LAMINATED CORES

The magnetic core of laminated sheets in the accelerator is one of the problems, since it causes a poor vacuum, thus inducing an electrical breakdown. Figure 9 shows the outgassing rates measured for laminations with insulating coatings. The surface coating was a quasi-inorganic material and had been thermally cured at a rather low temperature of 350C. It is to be noticed that the outgassing rates for closely and loosely stacked cores do not show any significant difference when the pumping period is as long as 100h, or more. Further, though pre-baking of the laminations is effective to shorten the pumping period, once exposed to atmospheric air with humidity, the outgassing rate again shows a larger value[17].

Probably, the adsorbed/absorbed water molecules on/in the coatings require an activation energy to desorbs, while, once desorbing, they can diffuse more easily, even in a narrow gap of several microns or less. This indicates that the coating materials dominate the pump-down characteristic. Indeed, stainless-steel laminations without any coatings showed much lower outgassing rates, even when stacked; also, lamination with inorganic coatings by high-temperature curing has a low rate.

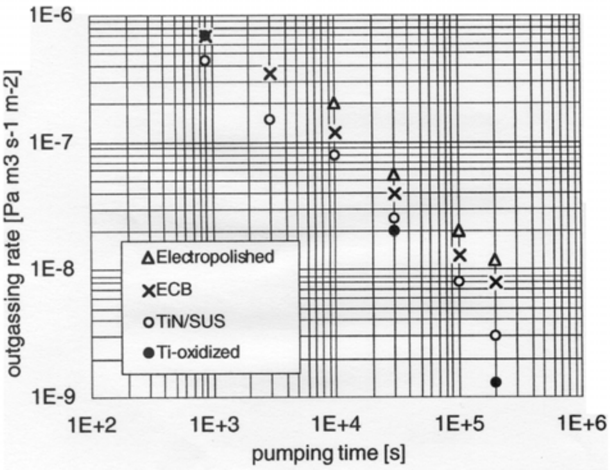

Figure 7 - Outgassing rate of stainless-steel test ducts measured by the conductance-modulation method. The as-received duct was treated by electropolishing

Since the rates shown in Fig.9 are presented in terms of the surface unit area of the sheet, we should take account of an areal effect. The rate measured for an uncoated stainless-steel sheet is in the range of 2 x 10^{-8} Pa m^3 s^{-1} m^{-2} at 100h pumping. However, the cube of the stacked laminations of 100 x 100 x 100 mm has a larger outgassing rate of 8 x 10^{-6} Pa m^3 s^{-1} m^{-2}, assuming that all of the gas is released from the cubic surface. This value is nearly close to that of a polyethylene bulk cube of the same size.

4.3. COAXIAL CABLES

Another problem concerns outgassing from electric wiring in a vacuum. There are several kinds of coaxial cables commercially available, which are not for special use in a vacuum. Some organic compounds, such as polyethylene, are used as insulators. A stainless steel sheathed coaxial cable with vacuum-sealed connectors at both extremities, having MgO powder inside the sheath is, on the contrary, expected to have a lower outgassing rate.

The outgassing rates of these coaxial cables are compared[18] in Fig.10 by unit length. A bridged-polyethylene insulated cable, electrically shielded by a copper mesh, shows large outgassing of 10^{-7} Pa m^3 s^{-1} m^{-1}. A fluorinated-ethylene-propylene insulated cable, shielded by Ag-plated copper mesh, has a lower rate of 10^{-9} Pa m^3 s^{-1} m^{-1}, but it is not suitable for use as accelerator components because of a lack of radiation resistance. A ceramic (SiO2)-coated aluminum wire, though it is an inorganic material, does not show a low rate, indicating porosity in the coatings. The stainless-steel sheathed coaxial cable has the lowest outgassing rate of any cables measured.

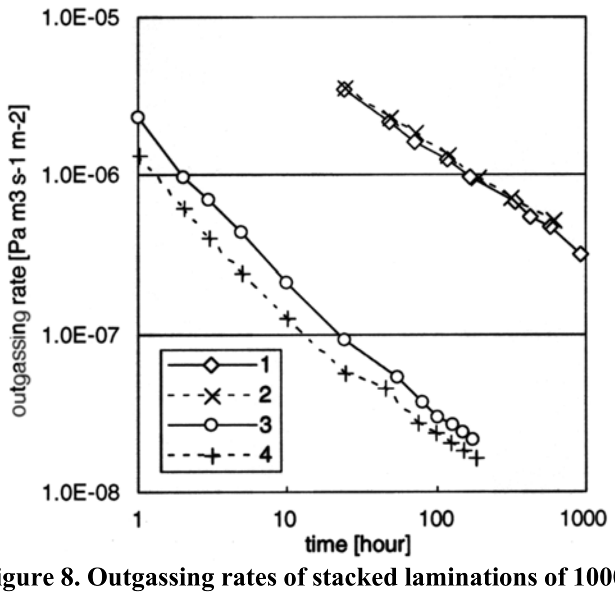

Figure 8. Outgassing rates of stacked laminations of 1000 sheets. The size of each lamination (0.1 mm thick) is 100 x 100 mm. 1 and 2 are the laminations of silicate iron with an insulating coating, stacked in compressed (about 2 μm of spacing) and uncompressed (0.1 mm of spacing) condition, respectively. 3 (compressed) and 4 (uncompressed) are the stainless-steel laminations without coatings

5. SUMMARY

Based on the results of an examination concerning the breakdown characteristics, the following are necessary when choosing materials and treating surfaces for use as accelerator vacuum components. As for oxygen-free-copper, the material specified by ASTM-F-68 as Class-1, having fewer voids, and consequently a smaller hydrogen content, shows better performance concerning breakdown strength. Degassing by in-vacuum annealing is effective to further increase the strength. Besides surface smoothness, it is also important to reduce any residual stresses of the electrodes by such processes as diamond turning. Also, in-situ cleaning by ion-beam sputtering had better be applied before conditioning. For aluminum, a new method of pit-free electropolishing gives a mirror-finished surface, which has a 200 nm thick oxide layer and is not porous. This surface shows high durability under a high electric field, indicating a stable layer. In the breakdown mechanism of alumina ceramics in rf windows, the electronic states in an oxygen vacancy plays an important role. An electron in F-center is excited to the conduction band, and then causes surface melting.

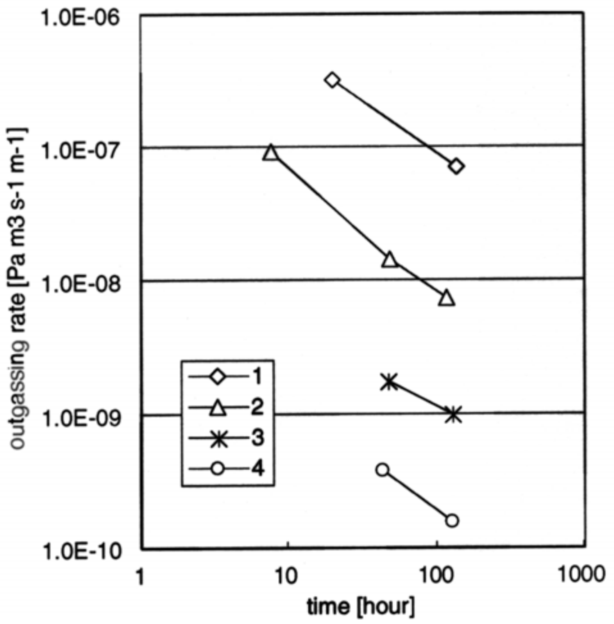

Figure 9 - Measured outgassing rate (per unit length) for electric cables. 1, Bridged-polyethylene insulated cable with Cu mesh shielding of 2 mm in dia; 2, SiO_2coated Al/Cu inner conductor with galss-fiber insulator, shielded by Cu mesh of 1.1 mm in dia; 3, Fluorinated ethylene-propyrene insulated cable with Ag/Cu mesh shield of 2 mm in dia; 4, Stainless-steel sheathed coaxial cable.

The material, having a low loss-tangent factor and not having a void nor a pre-existing F-center, should be chosen. It is also effective to suppress multipactoring in order to avoid a detrimental breakdown. The TiN coating on the alumina ceramic, having a short electron mean-free-path, reduces to emit secondary electrons generated in the alumina.
From the results of outgassing measurements of surface-treated stainless-steel, several methods are effective to reduce outgassing. An electrochemical-buffing method without using any large furnace or liquid reservoir is advantageous to apply to a large area; however, the surface is not as passivated as a TiN-coated surface. The outgassing rate of the magnetic core of laminations is found to depend not on the spacing distance between the laminations, but on the insulating coatings. Even when the insulation coating is cured by high temperature, consequently having a lower outgassing rate, the stacked core effectively gives a large amount of outgassing due to the large surface area. Several kinds of coaxial cables have been examined for vacuum use. A stainless-steel sheathed cable showed a lower outgassing rate than polyethylene insulated or ceramic-coated ones.

REFERENCES

1. NAGAI, Y. et. al., Vacuum **41** (1990) 2100.
2. KOBAYASHI, S. et. al., IEEE Trans. Dielectrics *EI* **4** (1997) 841.
3. BABA, Y. et. al., *Super Mirror-Flat Finishing of Metal Surfaces by Electrochemical Buffing*, Proc. XV Int. Symp. on Discharge and Electr. Insul. In Vacuum, ed. By D.Konig, Darmstadt, p3, 1992.
4. TAJIRI, K. et.al., JVST A **16** (1998) 1196.
5. KOBAYASHI, S. et. al.; Appl. Surf. Sci. **144-145** (1999) 118.
6. SAITO, Y. et. al., Rev. Sci. Instrum. **60** (1989) 1736.
7. YAMAGUCHI, S. et. al., IEEE Trans. NS **39** (1992) 278.
8. SAITO, Y. et. al., IEEE Trans. EI **24** (1989) 1029.
9. MICHIZONO, S. et. al., IEEE Trans. EI **28** (1993) 692.
10. MICHIZONO, S. et. al., JVST A **10** (1992) 1180.
11. SAITO, Y. et. al., IEEE Trans. EI **28** (1993) 566.
12. MICHIZONO, S. et. al., J. Vac. Soc. Japan **40** (1997) 436.
13. SATO, T. et. al., Appl. Surf. Sci. **144-145** (1999) 324.
14. TERADA, K. et. al.; JVST A **7** (1989) 2397.
15. SAITO, Y. et. al., Vacuum **53** (1999) 353.
16. SAITO, Y. et. al, Vacuum **60** (2001) 3.
17. SATO, Y. et. al., J. Vac. Soc. Japan **43** (2000) 962 (in Japanese).
18. KUBO, T. et. al., J. Vac. Soc. Japan **41** (1998) 217.